AGU PUBLICATIONS

Geophysical Research Letters

RESEARCH LETTER
10.1002/2017GL074394

Key Points:
- Local-scale latent heat advection is a previously undocumented source of energy for snowmelt
- Latent heat advection requires an upwind water vapor source
- Latent heat advection is an important snowmelt process in low relief areas where surface water storage during melt is likely

Correspondence to:
P. Harder,
phillip.harder@usask.ca

Citation:
Harder, P., Pomeroy, J. W., & Helgason, W. (2017). Local-scale advection of sensible and latent heat during snowmelt. *Geophysical Research Letters*, *44*. https://doi.org/10.1002/2017GL074394

Received 2 JUN 2017
Accepted 9 SEP 2017
Accepted article online 13 SEP 2017

Local-Scale Advection of Sensible and Latent Heat During Snowmelt

Phillip Harder[1], John W. Pomeroy[1], and Warren Helgason[1,2]

[1]Centre for Hydrology, University of Saskatchewan, Saskatoon, Saskatchewan, Canada, [2]Department of Civil, Geological, and Environmental Engineering, University of Saskatchewan, Saskatoon, Saskatchewan, Canada

Abstract The breakup of snow cover into patches during snowmelt leads to a dynamic, heterogeneous land surface composed of melting snow, and wet and dry soil and plant surfaces. Energy exchange with the atmosphere is therefore complicated by horizontal gradients in surface temperature and humidity as snow surface temperature and humidity are regulated by the phase change of melting snow unlike snow-free areas. Airflow across these surface transitions results in local-scale advection of energy that has been documented as sensible heat during snowmelt, while latent heat advection has received scant attention. Herein, results are presented from an experiment measuring near-surface profiles of air temperature and humidity across snow-free to snow-covered transitions that demonstrates that latent heat advection can be the same order of magnitude as sensible heat advection and is therefore an important source of snowmelt energy. Latent heat advection is conditional on an upwind source of water vapor from a wetted snow-free surface.

Plain Language Summary During snowmelt snow cover becomes heterogeneous and lateral transfer of energy between bare and snow surfaces is an important but underrepresented component of the surface energy balance. To date, there have been no observations of latent heat advection which is the energy transfer associated with evaporation from ponded melt-water and subsequent condensation upon downwind snow patches. This paper presents observations and a conceptual framework that is used to quantify this previously undocumented energy balance component. Latent heat advection can represent up to 33% of the snowmelt energy which has large implications for the snowmelt process. This work demonstrates that both sensible and latent heat advection processes need to be included in future snow modeling efforts in order to improve snowmelt predictions which have wide ranging water resource management implications.

1. Introduction

Snow-covered area declines, and snow cover becomes patchy during the course of snow ablation, significantly influencing snow-atmosphere interactions and snowmelt rates (Granger et al., 2006; Marsh & Pomeroy, 1996; Ménard et al., 2014; Pomeroy et al., 1998). The differences in energetics across snow and non-snow areas lead to a heterogeneous distribution of surface temperatures as snow is limited to a maximum of 0°C due to phase change. Air flow across patchy snowcover leads to local-scale sensible heat advection (H_A) to snow (Essery et al., 2006; Granger et al., 2002; Liston, 1995; Mott et al., 2013; Weisman, 1977); however, complimentary research on latent heat advection (LE_A) has not occurred.

Measuring advection is challenging, and direct observations of its impact on melt rates are recently demonstrated by Mott et al. (2011), who documented consistently greater melt rates on the leading edge of snow patches from repeat terrestrial laser scanning. Field studies to understand the processes describing advection are most frequently based upon observations of near-surface changes in air temperature (T_a) across surface transitions. Abrupt changes in surface temperature and humidity cause internal boundary layers to develop downwind of the transition (Garratt, 1990). Granger et al. (2002, 2006) demonstrated that internal boundary layers of T_a across snow free to snow transitions follow an established power law relationship with height and can be related to H_A through boundary layer integration. In complex terrain, internal boundary layer development may be impeded by atmospheric decoupling of the atmosphere from the snow surface which subsequently suppresses H_A (Mott et al., 2013). Because of challenges with observational approaches, modeling has been used to understand the possible energy and mass flows associated with advection. Early work by Weisman (1977)

applied mixing length theory to estimate advection to lakes and snow patches with the model implicitly accounting for both LE_A and H_A. Subsequent approaches have varied in complexity. A simple approach taken by Marsh and Pomeroy (1996) related bare ground sensible heat fluxes to areal average H_A via an advection efficiency term which relates to snow-covered area. The application of internal boundary layer integration (Essery et al., 2006; Granger et al., 2002) to tile models (Essery et al., 2006) while accounting for the fractal nature of snow cover (Shook et al., 1993) has provided another approach to estimate areal average estimates of advection. More complex approaches have employed atmospheric boundary layer models (Liston, 1995) and large eddy simulation (Mott et al., 2015) to quantify the nonlinear relationships between snow patch characteristics/geometry and advected energy. Numerical models provide the most detailed description of the processes but are constrained to idealized boundary conditions. The challenge in all observational or modeling approaches surveyed is that none are validated with actual observations of advection nor explicitly partition advected energy into sensible or latent heat components during snowmelt.

A simple alternative approach to quantify advection in turbulent flow, which does not require representations of internal boundary growth, stability, or surface roughness, is possible by consideration of the two-dimensional Reynolds-averaged scalar budget (Paw U et al., 2000)

$$\frac{\partial \overline{c}}{\partial t} + \overline{u}\frac{\partial \overline{c}}{\partial x} + \overline{w}\frac{\partial \overline{c}}{\partial z} + \frac{\partial}{\partial x}\left(\overline{u'c'}\right) + \frac{\partial}{\partial z}\left(\overline{w'c'}\right) = \overline{S}, \tag{1}$$

where c is the scalar of interest, t (s) is time, u (m s^{-1}) is horizontal wind speed, w (m s^{-1}) is vertical wind speed, x (m) is horizontal distance, z (m) is vertical distance, and S (scalar unit s^{-1}) is the scalar net source/sink rate. Overbars denote interval averages, while primes denote instantaneous deviations from interval averages. The terms, from left, represent storage, horizontal advection, vertical advection, horizontal turbulent flux divergence, and vertical turbulent flux divergence. Integrating equation (1) with respect to the profile depth results in a framework to quantify H_A (W m^{-2}) and LE_A (W m^{-2}) for the horizontal advection term from two-dimensional specific humidity (q: kg kg^{-1}) and T_a (°C) profiles to give (Kochendorfer & Paw U, 2011)

$$\int_{z=0}^{z_p} \rho C_p \overline{u}\frac{\partial \overline{T}}{\partial x} dz = H_A, \tag{2}$$

and

$$\int_{z=0}^{z_p} \rho L_v \overline{u}\frac{\partial \overline{q}}{\partial x} dz = LE_A. \tag{3}$$

In equations (2) and (3), z_p (m) is the profile depth of interest, ρ (kg m^{-3}) is the density of air, C_p (1,005 J kg^{-1} K^{-1}) is the specific heat capacity of air, and L_v (2.835 ×106 J kg^{-1}) is the latent heat of vaporization.

A comparable field experiment (Kochendorfer & Paw U, 2011) also examined vertical advection and turbulent fluxes across smooth (bare soil) to rough (1 m sorghum). These observations demonstrated that vertical advection is due to deceleration and upward motion of airflow in the sorghum canopy. For the relatively smaller change in roughness from a short crop stubble (rough) to snow (smooth), vertical advection will have a much smaller impact.

The overall objective of this study is to assess the role of H_A and LE_A from nonsnow surfaces to snow-covered surfaces during snowmelt with field observations.

2. Methodology

2.1. Site

The field site, situated near Rosthern, Saskatchewan, Canada (52.69°N, 106.45°W), is representative of the Canadian Prairie agricultural region. Topographic relief is limited, and the local landscape is interspersed

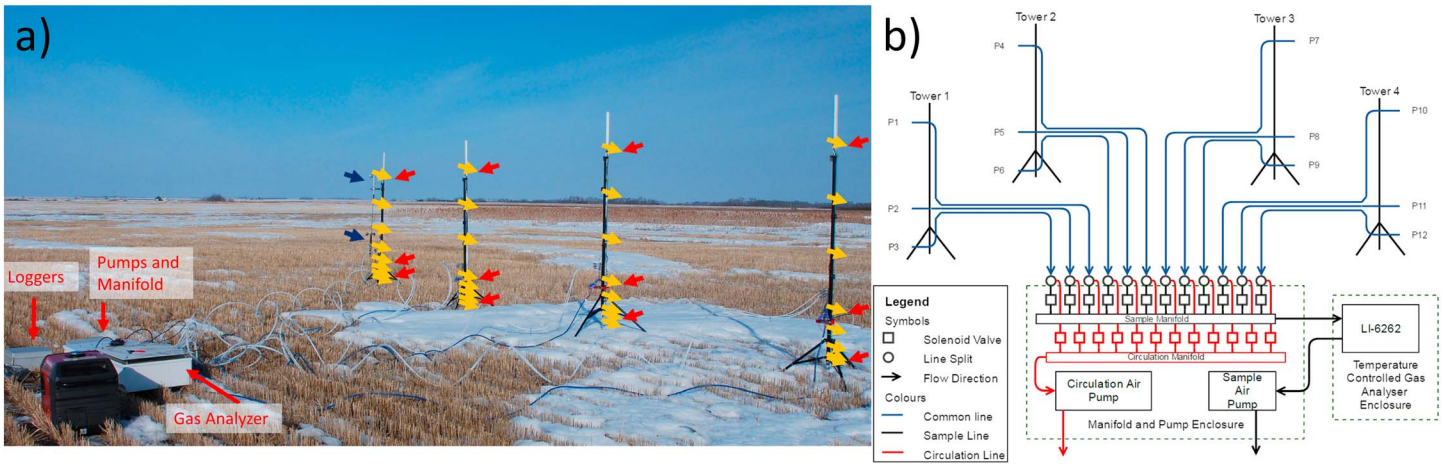

Figure 1. (a) Deployed atmospheric profile observation system. Sensors are spread over 4 mobile towers and include 2 three-cup anemometers (blue arrows), 32 fine wire thermocouples (yellow arrows) and 12 water vapor intakes (red arrows) that (b) are routed sequentially to a common gas analyzer.

with woodlands and wetlands. Maximum snow depth is typically less than 0.50 m, and the snow-covered area is patchy and dynamic during ablation (Pomeroy & Gray, 1995). Data were collected at the 65 ha study site during March 2015. The surface roughness was defined by the presence of standing wheat stubble which remained erect throughout the snow season. Stubble height was approximately 0.35 m on a tall stubble treatment and 0.15 m on a short stubble treatment.

2.2. Instrumentation

Profiles of T_a, q, and u are required to estimate advection following the framework conceptualized in equations (1) to (3). A mobile system, composed of sensors mounted on four towers, was developed for rapid deployment to surface transitions of interest (Figure 1a). Instrumentation was mounted on an adjustable rail to ensure consistent sensor heights relative to the surface. Wind speed was observed with two Met One 014A three-cup anemometers mounted on the upwind tower at 1.00 m and 2.00 m. Air temperature profiles were measured with 76.2 μm diameter Type-T fine wire thermocouples at 0.04 m, 0.08 m, 0.16 m, 0.32 m, 0.50 m, 1.00 m, 1.50 m, and 2.00 m on each tower.

Measurement of q was challenging due to the high accuracy required to detect small differences over short distances. A q profiling system was developed to route air from 12 intake ports (deployed at 0.08 m, 0.50 m, and 2.00 m on the four towers) to a common sensor, a LiCOR-6262 CO_2/H_2O gas analyzer (Li-6262). Figure 1b provides a schematic of the system. A dedicated air pump drew air through the manifold system and gas analyzer, while another pump circulated air through the remaining 11 lines to prevent in-line condensation and ensure representative air samples at the analyzer. Gas routing was controlled via a data logger that recorded q and the corresponding intake port at 1 s intervals. Tube lengths for all ports were 10 m; 1 L min^{-1} flow in a one-fourth inch tube gives an estimated 3 s travel time ignoring diffusion in these tubes. Lab testing showed consistent signal stabilization 5 s after port changes. To be conservative during deployments, the port was switched every 20 s with only the last 10 s retained for analysis. This gave a 4 min cycle to sample all 12 intakes. The Li-6262 gas analyzer was operated in an insulated, temperature-controlled enclosure and calibrated prior to deployment against a LiCOR-610 dew point generator.

The system was deployed over a variety of nonsnow to snow cover transitions with Tower 1 upwind of a snow-free to snow-covered transition, Tower 2 at the transition, and Towers 3 and 4 sequentially downwind of the transition. Analysis was limited to two unique periods of observation; conditions are summarized in Table 1 and spatial arrangement of towers and surface visualized in Figure 2. These met data quality requirements that include minimum wind speeds, wind direction alignment, sensor performance, and consistent sensor displacement with respect to surface. The 18 March observation period was characterized by an upwind uniform surface of wheat stubble exposed above a continuous snow cover that should correspond to negligible q and large T_a horizontal gradients that will lead to negligible LE_A and large H_A. In contrast,

Table 1
Summary of Mean Conditions During Observation Intervals

Attribute	Unit	18 March 2015	30 March 2015
Observation period		13:00–15:00	11:20–12:00
Number of analysis intervals		31	11
Stubble height	m	0.35	0.2
Tower spacing[a]	m	3.7, 3.1, 4.4	3, 3.6, 4.8
Array bearing	deg	161	271
Wind direction[b]	deg	166 (6.4)	274 (0.8)
Air temperature	°C	5.4	7.9
Snow temperature	°C	0.3	0.3
Relative humidity	%	60.0	72.1
Wind speed	m s^{-1}	1.6	6.4
Sensible heat[c]	W m^{-2}	−57.3	−58.4
Latent heat[c]	W m^{-2}	−22.2	−133.7
Net radiation	W m^{-2}	326.2	472.6
Stability[d]	-	−0.1	−0.007
Friction velocity	m s^{-1}	0.20	0.57

[a]Tower spacing is the distance between Towers 1 and 2, Towers 2 and 3, and Towers 3 and 4. [b]Bracketed values are the standard deviation. [c]Areal average turbulent terms from adjacent eddy covariance observations. [d]Stability parameter (z/Obhukov length) observed at 1.8 m from adjacent eddy covariance observations.

30 March was characterized by the upwind surface having wheat stubble exposed above patches of ponded water. The 30 March condition should lead to large q and T_a horizontal gradients and therefore both large H_A and LE_A.

Incoming radiation was observed with a Kipp and Zonen CNR1 net radiometer at a permanent reference station within 350 m of the deployed array. Outgoing longwave and shortwave terms were observed with a CGR3 pyrgeometer and a CMP6 pyranometer, respectively, at adjacent on-field stations within 50 m of the deployed array. Additional observations at the on-field stations include T_a and relative humidity at 1.65 m height with a shielded HMP45C212, snow surface temperatures with Apogee S-111 Infrared Radiometers, and ground heat flux beneath snow cover with Hukseflux self-calibrating heat flux plates. Eddy covariance (EC) instrumentation, Campbell Scientific CSAT3 Sonic anemometer for wind speed and ultrasonic temperatures and LiCOR 7500A open-path infrared gas analyzer for water vapor observations, quantified sensible and latent turbulent heat fluxes, friction velocity, stability, mean wind speed, and mean wind direction at a height of 1.8 m.

2.3. Data Analysis

To calculate the advection terms, following equations (2) and (3), the point observations of u, T_a, and q were integrated over the profile depth of interest. The $\overline{u}$ for the integrated profile depth was found by fitting observations to the classic logarithmic wind profile

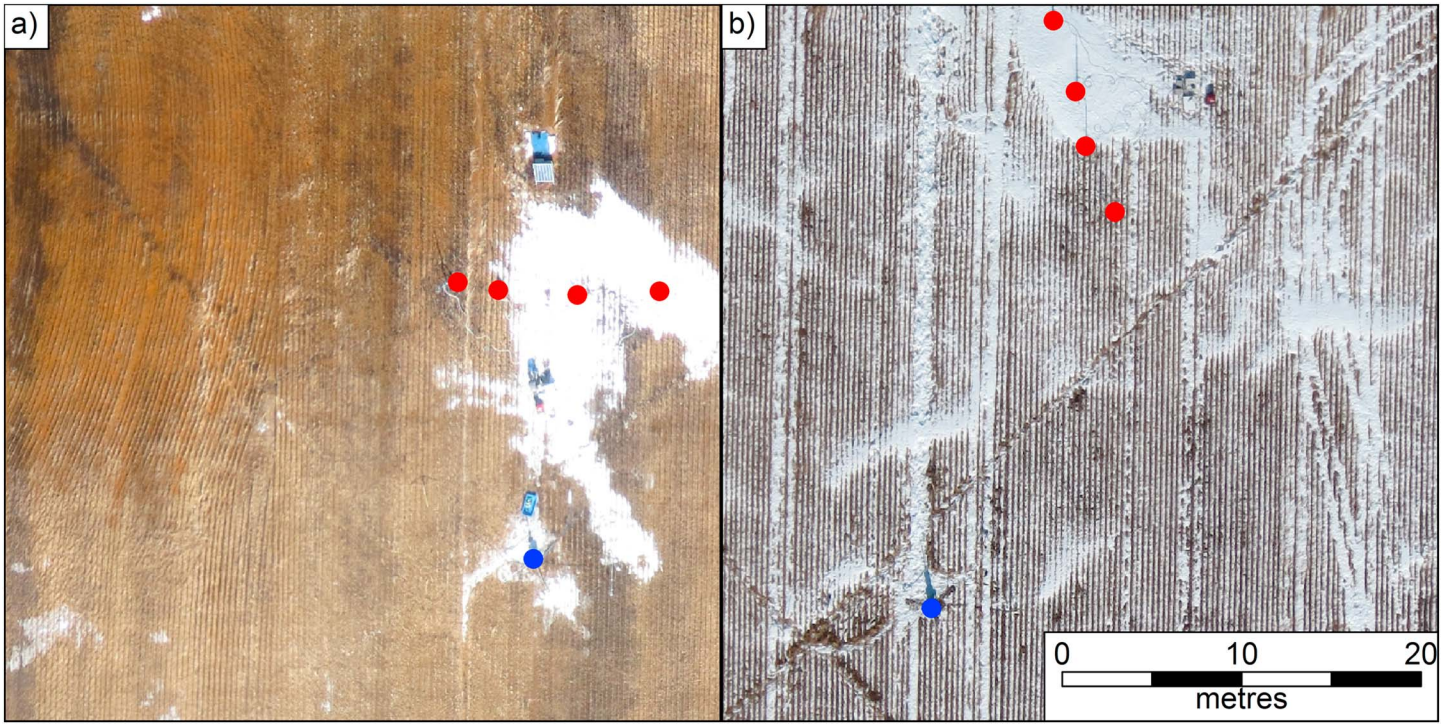

Figure 2. Unmanned aerial vehicle imagery of (a) 18 March 2015 and (b) 30 March 2015 deployments. Red points are locations of towers with Tower 1 upwind in nonsnow location, Tower 2 located at transition, and Towers 3 and 4 situated sequentially downwind over snow. Towers are in line with the prevailing wind direction over the observation interval. Blue dot is location of eddy covariance system and additional in-field instrumentation.

$$\overline{u} = \int_{z=0}^{z_m} \frac{\overline{u}^*}{k} \log\left(\frac{z + d_0}{z_0}\right) dz, \tag{4}$$

where z_m (m) is the height of the profile of interest and k is the von Kármán constant (0.4). The displacement height d_0 (m) and surface roughness z_0 (m) are estimated as

$$d_0 = 0.67 h_v \tag{5}$$

and

$$z_0 = 0.12 h_v, \tag{6}$$

respectively, where h_v (m) is the height of vegetation. Mean interval friction velocity ($\overline{u}^*$: m s^{-1}) is calculated as

$$\overline{u}^* = k(\overline{u}_2 - \overline{u}_1) \ln\left(\frac{z_2 - d_0}{z_1 - d_0}\right)^{-1}, \tag{7}$$

with the mean interval wind speed observations $\overline{u}_2$ and $\overline{u}_1$ (m s^{-1}) observed on Tower 1 at heights z_2 (2 m) and z_1 (1 m), respectively. The logarithmic wind profile was not corrected for stability. The near-surface atmosphere, from EC observations at 1.8 m, was near neutral during observation intervals (Table 1). In addition, the stability corrections are invalid at heights less than $41 \cdot z_0 + d_0$ (Brutsaert & Parlange, 1992) which corresponds 1.1 m for a 0.20 m stubble surface; this is greater than the 0.5 m profile depths of interest.

Other advection studies have interpolated between profiles by fitting predefined curve functions to observations (Essery et al., 2006; Kochendorfer & Paw U, 2011). Due to the diverse profiles encountered, and a limited number of q observation levels, curve fitting with a predefined function is inappropriate. Rather, a layer depth-weighted mean was applied over the integration height

$$\overline{c} = \Sigma_{i=1}^{i=n-1} \left(\frac{c_{i+1} + c_i}{2}\right)(z_{i+1} - z_i) dz^{-1}, \tag{8}$$

where c_i is the ith scalar at measurement heights i from the surface to the top of the profile integration height of interest, n *is* the number of observation points, and dz (m) is the profile depth of interest. Over the downwind snow surfaces surface T_a was observed from adjacent snow surface temperature measurements and surface q was estimated assuming saturation of the surface air. The upwind towers are more complicated as the surface is not uniform snow. Therefore, surface T_a was estimated by linear interpolation of the three lowest observations to the surface. Surface q was estimated by assuming saturation at the interpolated T_a.

2.4. Instrumentation Uncertainties

Advection calculations require instrumentation that can observe small gradients in T_a and q in two dimensions. Unshielded fine wire thermocouples were selected for measuring T_a due to their fast response time. Despite the small thermocouple diameters, these sensors will experience radiative heating that varies with the wind speed profile. The change in thermocouple temperature difference from T_a due to expected wind speed differences at heights from 0.04 to 0.5 m was estimated using Campbell (1969) to be less than 0.14 K so the observations are assumed to represent actual gradients. The largest uncertainty of the q observations is due to intermittent port sampling. The occurrence of q or T_a anomalies/plumes from variable upwind footprints could complicate profile interpretations. To minimize the influence of such anomalies, analysis was limited to periods with wind directions aligned with the towers to limit upwind footprint variability and ensure any anomalies impacted all towers. Unlike intermittent q observations, the T_a observations are continuous and examination of these did not identify anomalies that could skew results. The error of the absolute humidity signal of the LI-6262, according to the manufacturer specifications, is 0.01 g m^{-3}. Since gradient calculations require two observations the differences should be greater than combined error of 0.02 g m^{-3}; 85% of the differences observed were greater than this threshold.

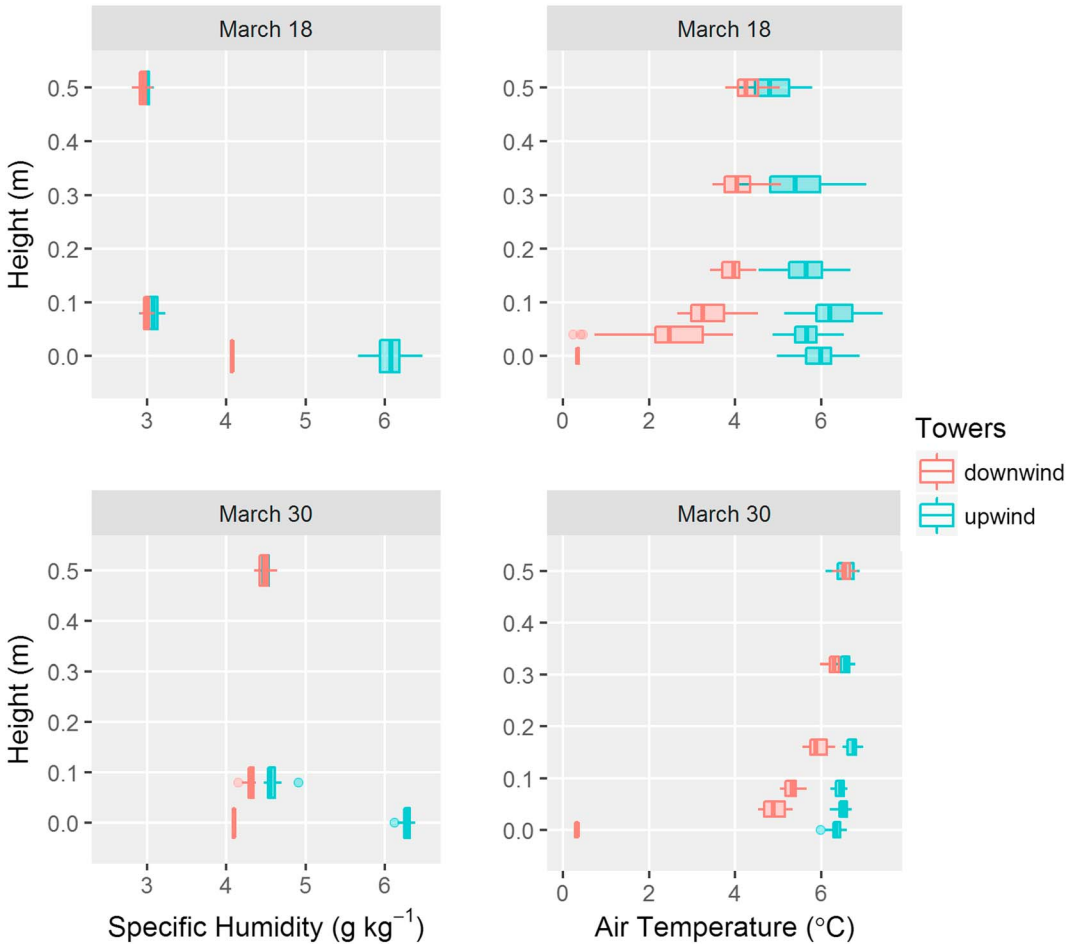

Figure 3. Specific humidity and air temperature observations versus height grouped as box plots upwind and downwind of a snow surface transition for (top row) 18 March and (bottom row) 30 March 2015 observations periods.

3. Results and Discussion

3.1. Air Temperature and Water Vapor Profiles

The influence of a surface transition upon q and T_a profiles (Figure 3) is evident in upwind and downwind observations showing relatively large differences compared to the small range in observations between towers of the same surface. These differences are clearly associated with rapid change in atmospheric profiles on the leading edge of the snowpack between Towers 2 and 3. The difference in profiles diminishes at heights near 0.50 m which correspond to the development of an internal boundary layer and the formation of a blending height (Granger et al., 2006, 2002).

Despite the limited sample heights on each profile, the observed 0.08 m and assumed surface q values are always greater upwind than downwind of the bare snow edge; the differences are minimal at 0.50 m. The decrease in q over a snow transition on 30 March validates the concept that q decreases over snow-covered fetch because of condensation from the moisture laden warmer air to the colder, relatively dry, snow surface. In contrast the q profiles on 18 March reflect a sublimation condition both upwind and downwind. Advection of LE_A will not occur in this situation, but the relatively moist upwind q profile will still act to suppress turbulent exchange of latent heat over snow; this provides a mechanism for why snowmelt latent heat fluxes are routinely observed to be small in this region (Granger & Male, 1978; Pomeroy & Essery, 1999; Pomeroy et al., 1998). The small differences in q between the towers at the 0.50 m and 2.00 m heights (not shown) support the hypothesis of negligible differences in the well-mixed air mass above the internal boundary layer. The q profiles show much smaller differences early in the melt season (18 March) when soils were frozen near the

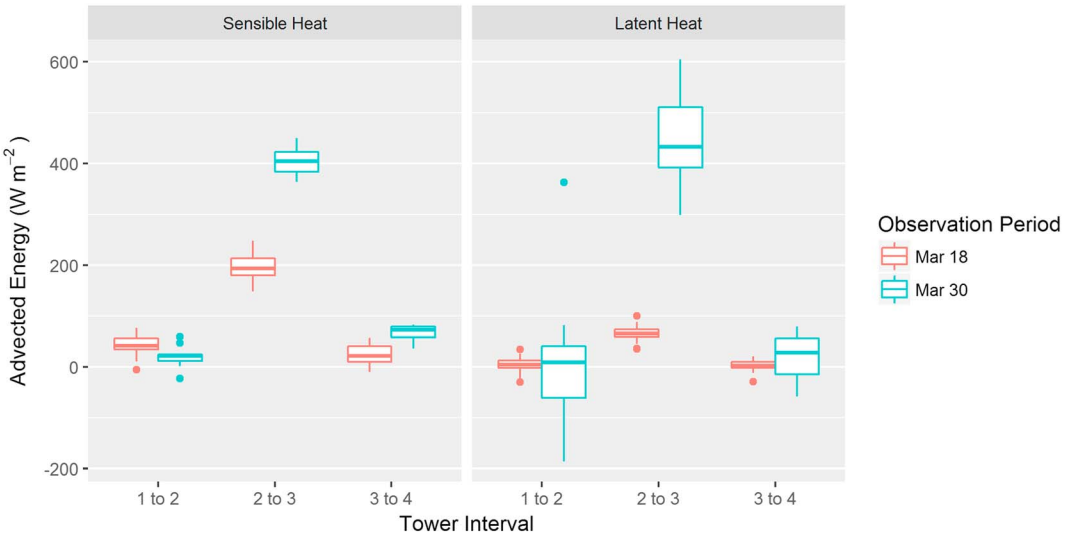

Figure 4. Sensible and latent heat advection estimates between each set of towers. The box plots summarize the 4 min advection estimates for the respective observations periods.

surface and ponded water was absent. Later in the melt period, 30 March, the wet, thawed soil surface and ponded meltwater due to a frost table just below the surface provided vapor sources that drive the development of larger q gradients.

3.2. Advection Estimation

Advection terms were calculated using gradients between each set of towers so the advection flux could be attributed to a specific tower interval (Figure 4). The T_a and q profiles are temporally dynamic which leads to uncertainty in the advection estimates as shown by the ranges of estimates in Figure 4. Mean behavior shows negligible H_A and LE_A between Towers 1 and 2 suggesting that the air masses are relatively well mixed and in equilibrium with the upwind surface. Towers 2 to 3 interval, the leading edge of the snow patch, consistently has the greatest fluxes. The H_A and LE_A for Towers 3 to 4 interval, farther downwind of the edge, are predominantly negligible. During the ideal LE_A period, 30 March, when a strong wind blew from an upwind area of ponded water and wet soil over a snow transition, the mean LE_A was 446 W m^{-2} over the leading edge which is a similar magnitude to the corresponding mean H_A of 404 W m^{-2}. The relatively small LE_A contribution over the leading edge during the 18 March situation is negligible once the uncertainty range is considered.

The measurement of both H_A and LE_A contributions to snowmelt has not previously been reported; the observation that these terms may occur at similar large magnitudes is novel. These estimates reiterate that advection terms are most important on the leading edge of a snow patch as advection energy declines with the downwind development of equilibrium profiles.

3.3. Snowmelt Energy Balance Implications

To understand the snowmelt implications of LE_A and H_A on the leading edge of a snow patch, consider the melting snow surface energy balance (Gray & Male, 1981)

$$Q = R_{\text{net}} + H_A + LE_A + G, \tag{9}$$

where Q (W m^{-2}) is the net energy available for snowmelt, R_{net} (W m^{-2}) is the net radiation, and G (W m^{-2}) is the ground heat flux. This energy balance has been simplified by neglecting changes in snowpack internal energy and energy advected by rainfall. The net radiation term is the single largest energy input to the snow, followed closely by H_A and LE_A. Observed G was negligible as available energy was going into melting snow. H_A and LE_A, as a percent of snowmelt energy, were 33% and 11%, respectively, on 18 March and 31% and 33%, respectively, on 30 March. The net melt energy on the leading edge of a snowpack results in melt rates of 6.3 mm h^{-1}and 14.2 mm h^{-1} for 18 March and 30 March, respectively.

Rather than explicitly observe the H_A and LE_A terms on the leading edge of a snowpack, many observational campaigns rely on EC approaches to constrain the areal average turbulent terms of the energy balance. In this campaign, the areal average sensible and latent heat observations from adjacent EC sensors show energy fluxes away from the surface. This demonstrates the inappropriateness of EC to estimate the snowmelt energy balance of patchy snow, and consideration of H_A and LE_A is required to properly estimate the spatial variability of snowmelt.

Contrasting 18 and 30 March demonstrates that LE_A requires an upwind wetted surface as a source of q. Upwind wetted surfaces that can form sources of q are often found in flat areas with restricted infiltration that permit ponding of meltwater near snow patches. Conditions that favor the ponding of meltwater are frozen well-saturated soils and the presence of depressional storage to hold meltwater runoff in place. These conditions are often met in prairie, grassland, or tundra regions which are also characterized by patchy snow cover where H_A has been extensively documented (Granger et al., 2002; Marsh & Pomeroy, 1996; Shook & Gray, 1997). Model results suggest that advected energy can increase sensible heat fluxes in flat environments by about 50% over the first several meters on the leading edge of snowpack (Essery et al., 2006). The Essery et al. (2006) model results for sensible heat are similar to the H_A results of this study and increase confidence in the experimental design and the LE_A results. In contrast, sloping soils found in mountain environments will minimize the formation of ponded melt water on the surface. Sources for LE_A in mountains include concave surfaces that can hold water, but fluxes from these locations might be limited by lower wind speeds and cold stable air pools (Mott et al., 2011, 2013, 2015). The contribution of LE_A is not expected to be large during rain-on-snow events due to large latent heat sources from the already damp atmosphere (Pomeroy et al., 2016).

4. Conclusions

The energy balance of heterogeneous snow covers has long been recognized to be complicated by the advection of sensible heat from snow-free to snow-covered surfaces. However, the concomitant advection of latent heat from ponded water to snow patches has not been considered as a snowmelt energy source. Examination of T_a profiles over snow-free to snow-covered transitions reconfirms that H_A, driven by surface temperature heterogeneity, is a large source of energy available for snowmelt. The q profiles show that LE_A can also be substantial but is conditional upon the presence of upwind ponded water and/or wet exposed soils. Under conditions with wet upwind surfaces, the LE_A term was calculated to account for 33% of the net energy available for melt at the leading edge of a snow patch. This was on the same order as the corresponding H_A flux which accounted for another 31% of the net available energy melt. Thus, proper consideration of both sensible and latent heat advection fluxes is required to predict spatial melt rates in environments with patchy snow cover. The dependence of LE_A upon upwind wetted surface q sources means that its overall contribution to snowmelt depends upon the spatial arrangement of surface features, meteorological conditions, soil properties, and antecedent conditions.

Acknowledgments
This work was funded by the Natural Sciences and Engineering Research Council of Canada through Discovery and Research Tools and Instruments grants, the Changing Cold Regions Network, and the Canada Research Chairs programme. Data are available from the corresponding author upon request. Field and technical assistance from Bruce Johnson, Chris Marsh, Kevin Shook, and Michael Schirmer is gratefully acknowledged.

References

Brutsaert, W., & Parlange, M. B. (1992). The unstable surface layer above forest: Regional evaporation and Heat flux. *Water Resources Research*, *28*(12), 3129–3134. https://doi.org/10.1029/92WR01860

Campbell, G. S. (1969). *Measurement of Air Temperature Fluctuations with Thermocouples*. New Mexico: White Sands Missile Range.

Essery, R., Granger, R. J., & Pomeroy, J. W. (2006). Boundary-layer growth and advection of heat over snow and soil patches: Modelling and parameterization. *Hydrological Processes*, *20*(4), 953–967.

Garratt, J. R. (1990). The internal boundary layer—A review. *Boundary Layer Meteorology*, *50*, 171–203.

Granger, R. J., & Male, D. H. (1978). Melting of a prairie snowpack. *Journal of Applied Meteorology*, *17*, 1833–1842.

Granger, R. J., Essery, R., & Pomeroy, J. W. (2006). Boundary-layer growth over snow and soil patches: Field observations. *Hydrological Processes*, *20*(4), 943–951.

Granger, R. J., Pomeroy, J. W., & Parviainen, J. (2002). Boundary-layer integration approach to advection of sensible heat to a patchy snow cover. *Hydrological Processes*, *16*(18), 3559–3569.

Gray, D. M., & Male, D. H. (1981). *Handbook of Snow: Principles, Processes, Management, and Use*. Toronto, Canada: Pergamon Press.

Kochendorfer, J., & Paw U, K. T. (2011). Field estimates of scalar advection across a canopy edge. *Agricultural and Forest Meteorology*, *151*(5), 585–594. https://doi.org/10.1016/j.agrformet.2011.01.003

Liston, G. E. (1995). Local advection of momentum, heat and moisture during the melt of patchy snow covers. *Journal of Applied Meteorology*, *34*, 1705–1715.

Marsh, P., & Pomeroy, J. W. (1996). Meltwater fluxes at an Arctic forest—Tundra site. *Hydrological Processes*, *10*(10), 1383–1400.

Ménard, C. B., Essery, R., & Pomeroy, J. (2014). Modelled sensitivity of the snow regime to topography, shrub fraction and shrub height. *Hydrology and Earth System Sciences*, *11*(6), 2375–2392. https://doi.org/10.5194/hessd-11-223-2014

Mott, R., Egli, L., Grünewald, T., Dawes, N., Manes, C., Bavay, M., & Lehning, M. (2011). Micrometeorological processes driving snow ablation in an Alpine catchment. *The Cryosphere*, *5*(4), 1083–1098. https://doi.org/10.5194/tc-5-1083-2011

Mott, R., Gromke, C., Grünewald, T., & Lehning, M. (2013). Relative importance of advective heat transport and boundary layer decoupling in the melt dynamics of a patchy snow cover. *Advances in Water Resources*, *55*, 88–97. https://doi.org/10.1016/j.advwatres.2012.03.001

Mott, R., Lehning, M., & Daniels, M. (2015). Atmospheric flow development and associated changes in turbulent sensible heat flux over a patchy mountain snow cover. *Journal of Hydrometeorology*, *16*, 1315–1340. https://doi.org/10.1175/JHM-D-14-0036.1

Paw U, K. T., Baldocchi, D. D., Meyers, T. P., & Wilson, K. B. (2000). Correction of eddy-covariance measurements incorporating both advective effects and density fluxes. *Boundary-Layer Meteorology*, *97*(3), 487–511. https://doi.org/10.1023/A:1002786702909

Pomeroy, J. W., & Essery, R. (1999). Turbulent fluxes during blowing snow: Field tests of model sublimation predictions. *Hydrological Processes*, *13*(18), 2963–2975.

Pomeroy, J. W., & Gray, D. M. (1995). *Snow Accumulation, Relocation and Management*, Science Report No. 7. Saskatoon, SK: National Hydrology Research Institute, Environment Canada.

Pomeroy, J. W., Fang, X., & Marks, D. G. (2016). The cold rain-on-snow event of June 2013 in the Canadian Rockies—Characteristics and diagnosis. *Hydrological Processes*, *30*, 2899–2914. https://doi.org/10.1002/hyp.10905

Pomeroy, J. W., Gray, D. M., Shook, K., Toth, B., Essery, R. L. H., Pietroniro, A., & Hedstrom, N. (1998). An evaluation of snow accumulation and ablation processes for land surface modelling. *Hydrological Processes*, *12*, 2339–2367.

Shook, K., & Gray, D. M. (1997). Snowmelt resulting from advection. *Hydrological Processes*, *11*, 1725–1736.

Shook, K., Gray, D. M., & Pomeroy, J. W. (1993). Geometry of patchy snowcovers. In *50th Annual Eastern Snow Configuration* (pp. 89–98). Quebec City.

Weisman, R. N. (1977). Snowmelt: A two-dimensional turbulent diffusion model. *Water Resources Research*, *13*(2), 337–342. https://doi.org/10.1029/WR013i002p00337